CHEMICAL ENGINEERING TRANSACTIONS
VOL. 70, 2018
A publication of AIDIC
The Italian Association of Chemical Engineering
Online at www.aidic.it/cet
Guest Editors: Timothy G. Walmsley, Petar S. Varbanov, Rongxin Su, Jiří J. Klemeš

ISBN 978-88-95608-67-9; **ISSN** 2283-9216
DOI: 10.3303/CET1870067

Counter-Current Gas-Liquid Film Cross-Flow for the Staggered Tube Bundles in Closed Wet Cooling Towers

Xiaocui Xie, Chang He, Bingjian Zhang, Qinglin Chen*

School of Chemical Engineering and Technology/Guangdong Engineering Centre for Petrochemical Energy Conservation, Sun Yat-Sen University, Guangzhou 510275, Guangdong
chqlin@mail.sysu.edu.cn

This work establishes a three-dimensional CFD model that is capable of describing the counter-current air-water flow across a staggered tube bundle in a bench-scale wet cooling tower (CWCT) by combining the VOF multiphase method and the SST *k-ω* turbulence model. One important feature of the proposed model is that it investigates the interaction mechanisms among multiple tubes in the staggered tube bundle, which can reduce the gap between simulation and experiment. Through adding the air-water shear force term and water evaporation equation in the model, the effects of the spray density and the inlet air velocity on the falling film flow mode, air temperature in CWCT were studied. The numerical results show that, the inlet air velocity can largely influence the flow mode in CWCT. Under the spray density of 0.048 $kg \cdot m^{-1} \cdot s^{-1}$ and 0.060 $kg \cdot m^{-1} \cdot s^{-1}$ in which condition the Re_w is greater than 288, the falling film flow develops into column mode. The air temperature changes logarithmically along height direction, and their increase rates enlarge with the increment of spray water, but decrease with the increase of $u_{a,in}$. These results provide an insight into the complex mechanisms of heat-mass transfer for CWCTs.

1. Introduction

Closed wet cooling towers (CWCTs) possess remarkable advantages over conventional open wet cooling towers in water saving, less plume generation, high thermal efficiency, and no pollution to the process fluid and so on (Smith, et al., 2011). The heat transfer process from spray water to air consists of the sensible heat transfer driven by temperature difference and the latent heat produced by water evaporation. Therefore, the heat and mass transfers involved in the CWCTs mainly include three sub-processes in series: from process fluid to tube wall, from the tube wall to falling film, and from the spray water to air. These complex transfer processes lead to a number of challenges in model prediction, parametric analysis, mechanism investigation, and system optimization of CWCTs.

Motivated by both the advantages and challenges, substantial experimental and thermodynamic studies on CWCTs in the past have resulted in various empirical relations or correlations associated the flow behavior and thermo-hydraulic performances (Hasan and Siren, 2003). However, large-size experimental studies are usually capital-intensive and time-consuming, thus most of these experiments are implemented on simplified CWCTs that results in a limited range of applicability. That is, empirical finding or correlation is only applicable to the specific conditions under which it was developed. By contrast, numerical studies not only are easy to implement under any boundary conditions, but also can reveal details of heat and mass transfer processes that are difficult to measure in experiments. 2-D and 3-D models have been developed for the numerical simulation of gas-liquid flow behavior outside tubes, attributed to the significance of falling film flow mode and film distribution (Chen, et al., 2015). Because of the good ability of catching gas-liquid two-phase interface, the VOF model has been universally utilized in investigations of multiphase flow (Ding et al., 2013), and becomes the predominated CFD model employed in simulation of gas-liquid two-phase flow and heat transfer in evaporative heat exchangers such as CWCT.

Owing to the viscosity of fluid and velocity difference between gas-liquid two-phase flows, the shear force would affect the falling film distribution and heat transfer form tube wall to falling film and air. While the latent heat transfer caused by water evaporation accounts for a large proportion of overall heat transfer in CWCT.

Please cite this article as: Xie X., He C., Zhang B., Chen Q., 2018, Counter-current gas-liquid film cross-flow for the staggered tube bundles in closed wet cooling towers , Chemical Engineering Transactions, 70, 397-402 DOI:10.3303/CET1870067

Therefore, the air-water shear force and water evaporation in CWCT could not be ignored in numerical simulation. Under the effect of shear force, the falling film distribution highly differs from that without counter-current gas flow, and the film thickness of the lower perimeter of tube is typically affected. On consideration of mass flow rate of water evaporating to vapor, Fiorentino and Starace (2014) observed that the falling film thickness increase first and the sharply decrease along circumferential direction. Moreover, the air humidity changes along height direction and has a greater value near the tubes, while the overall heat transfer coefficient decreases with the increment of inlet air humidity. Considered the water evaporating rate, the trade-off curve of flow modes from droplet to stable sheet with 2-D model of staggered tube bundle had been obtained (Fiorentino and Starace, 2016). Summarizing the present numerical simulation, substantial researches concentrate on the falling film distribution outside tubes and flow mode transitions and analyze the effect of water evaporation on film thickness, film temperature and total heat transfer with two-dimensional model. However, investigating the air temperature, heat transfer and mass transfer in CWCT, using a rigorous and well-validated three-dimensional model, is hardly reported in the open literature in spite of its great importance.

Motivated by above investigations, this work establishes a three-dimensional numerical model with helps of the VOF multiphase model and SST *k-ω* turbulence model in Fluent software. According to the engineering practice, the spray density and inlet air velocity range from 0.010 to 0.060 $kg \cdot m^{-1} \cdot s^{-1}$ and 1.0 to 3.5 $m \cdot s^{-1}$, respectively. The air-water shear force and diffusion of water vapor were added in the momentum equation and mass equation, respectively, to study the effects of spray density and inlet air velocity on flow mode and air temperature in CWCT.

2. Numerical models

2.1 Geometry model and mesh generation

Based on the experimental apparatus shown in Figure 1 (Xie et al., 2017), the three dimensional geometry model was established as depicted in Figure 2. This model consists of a unit of staggered tube bundle of equilateral-triangular arrangement, and only half of the tubes both along the tube axial direction and circumferential direction are chosen due to the symmetry of geometry.

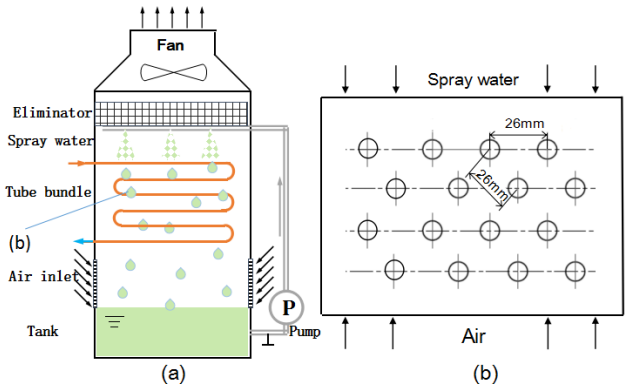

Figure1: Sketch of (a) the utilized bench-scale CWCT and (b) cross section of a tube bundle

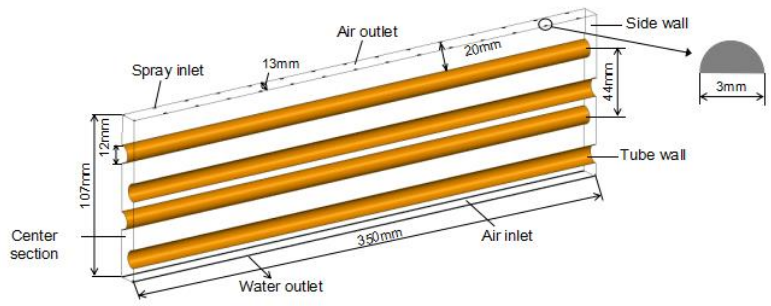

Figure 2: The three-dimensional geometry

Prior to applying this mesh in the numerical simulation, the mesh-independence is confirmed by comparing five different sizes of hexahedral mesh including 4.8×10^5, 8.2×10^5, 11.0×10^5, 14.0×10^5, and 16.0×10^5 under the same simulation conditions. Under the same conditions, the outlet air humidity acquired by five different meshes is shown in Figure 3. It can be observed that the outlet air humidity differences of the three models with large mesh number are less than 5 %. Therefore, considering the computational cost, the model with 1,100,000 mesh number is accurate enough for the numerical study. Figure 4 shows the structured mesh, the flow domain of water and the region near the tube wall adopt refined mesh.

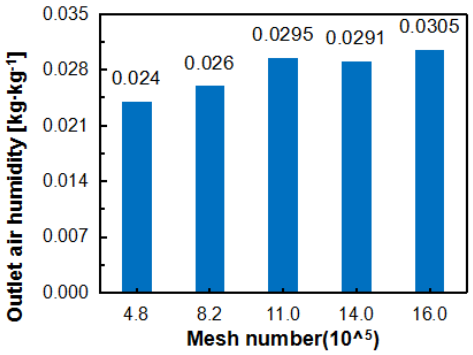

Figure 3: The outlet air humidity under five models of different mesh number

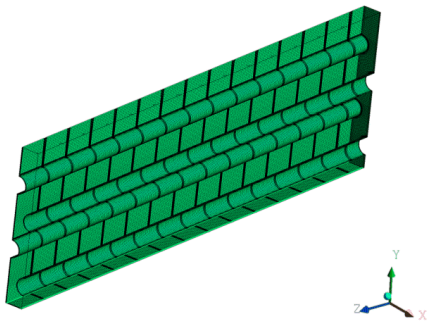

Figure 4: The structured mesh

3. Numerical results and discussion

3.1 Model validation

As a transient model, the independence of time step should be validated firstly. In this CWCT model, the outlet air humidity ($\omega_{a,out}$) of staggered tube bundle predominantly affected by falling film distribution and inlet air temperature can reflect the overall performance of heat-mass transfers outside tubes. Under the given air velocity ($u_{a,in}$=1.6 m·s^{-1}) and spray density (Γ=0.035 kg·m^{-1}·s^{-1}), four time steps (1.0×10^{-4}s, 5.0×10^{-5}s, 2.5×10^{-5}s, and 1.0×10^{-5}s) have been tested, and the results listed in Table 1 show that the maximum difference among the obtained $\omega_{a,out}$ is less than 5.5%. In order to reconcile the computational accuracy and burden, the time step of 5.0×10^{-5} s is selected in this numerical calculation.

Table 1: The simulation values of outlet air humidity under different time step

time step [s]	1×10^{-4}	5×10^{-5}	2.5×10^{-5}	1×10^{-5}
outlet air humidity [kg·kg-1]	0.0302	0.0295	0.0291	0.0286

3.2 The effect of spray density and inlet air velocity on flow mode

The spray density and inlet air velocity would affect the falling film flow, namely the flow mode, which determines the falling film thickness distribution along circumferential and axial directions. This changes the wetting area of tubes and contact area between water and air (José and Ángel, 2014), thus affecting the heat and mass transfer processes in CWCT. When the inlet air velocity is 1.6 m·s^{-1}, the flow modes under five different spray density are plotted in Figure 5 (a~e). Increasing the spray density from 0.010 to 0.060 kg·m^{-1}·s^{-1}, the falling film flow modes changes from droplet to droplet-column and column. In order to acquire the transition values of droplet to droplet-column and column under different spray density, more simulations have been adopted. With a more accurate correlation derived by Wang and Jacobi (2014), the critical transition values of droplet to droplet-column and droplet-column to column are obtained with spray water Reynolds number Re_w, Galileo number G_a and dimensionless tube spacing (s/ξ) as following

From droplet to droplet-column $$Re_w = 0.0548 Ga^{0.25}(s/\xi)^{0.5} \quad (1)$$

Corresponding transition value $$Re_w = 125 \quad (2)$$

From droplet-column to column $Re_w = 288$ (3)

Corresponding transition value $Re_w = 0.126Ga^{0.25}(s/\xi)^{0.5}$ (4)

The Re_w is smaller than 125 at the spray density of 0.010 kg·m^{-1}·s^{-1}, and water droplet falls down from the first tube of the bundle. When increasing the spray density to 0.024 kg·m^{-1}·s^{-1} and 0.035 kg·m^{-1}·s^{-1}, corresponding values of Re_w are greater than 125 but below 288, part of water flows continuously from upper tube to the below. Moreover, under the spray density of 0.048 kg·m^{-1}·s^{-1} and 0.060 kg·m^{-1}·s^{-1} in which condition the Re_w is greater than 288, all water flows successively down the first tube and the falling film flow develops into column mode.

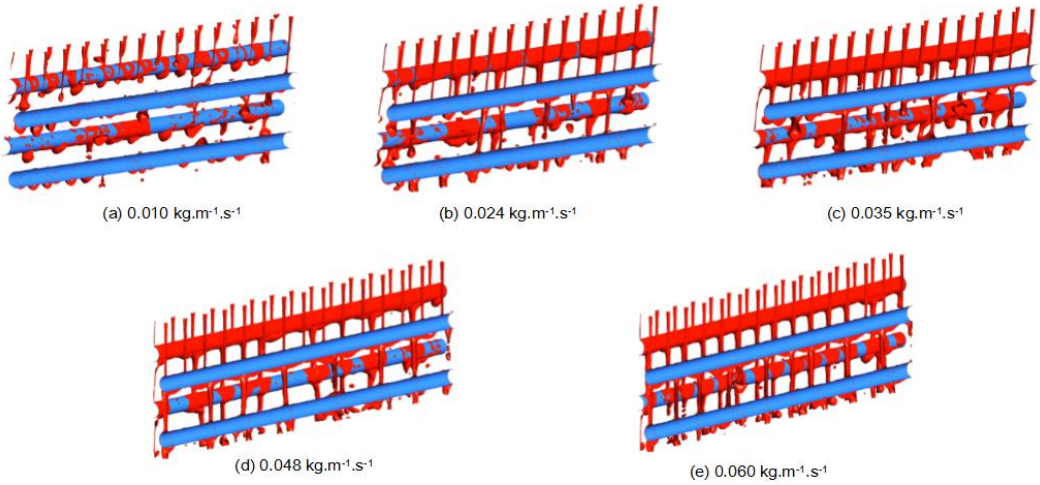

Figure 5: The influence of spray density on flow modes under the inlet air velocity of 1.6 m·s^{-1}

On the other hand, maintaining the spray density at 0.060 kg·m^{-1}·s^{-1}, the flow modes under three different inlet air velocity are shown in Figure 6(a~e). When increasing the inlet air velocity, the column mode changes to droplet-column and droplet, and transition values of air Reynolds number Re_a are obtained as given by Eq. (5-8).

From droplet to droplet-column $Re_w = 1.05Ga^{0.25}(s/\xi)^{0.5}$ (5)

Corresponding transition value $Re_w = 2595$ (6)

From droplet-column to column $Re_w = 1.88Ga^{0.25}(s/\xi)^{0.5}$ (7)

Corresponding transition value $Re_w = 4304$ (8)

Similarly, the Re_a is smaller than 2595 at the inlet air velocity of 1.0 m·s^{-1} and 2.2 m·s^{-1}, respectively, it could be seen that the falling film flows are column mode. The droplet-column mode occurs as the inlet air velocity increases to 2.2 and 2.8 m.s^{-1}, doe to that the corresponding values of the Re_a are between 2595 and 4304. While the Re_a is greater than 4304 and the falling film flow becomes droplet mode at the inlet air velocity of 3.5 m·s^{-1}. These changes indicate that the inlet air velocity can also largely influence the flow mode in CWCT.

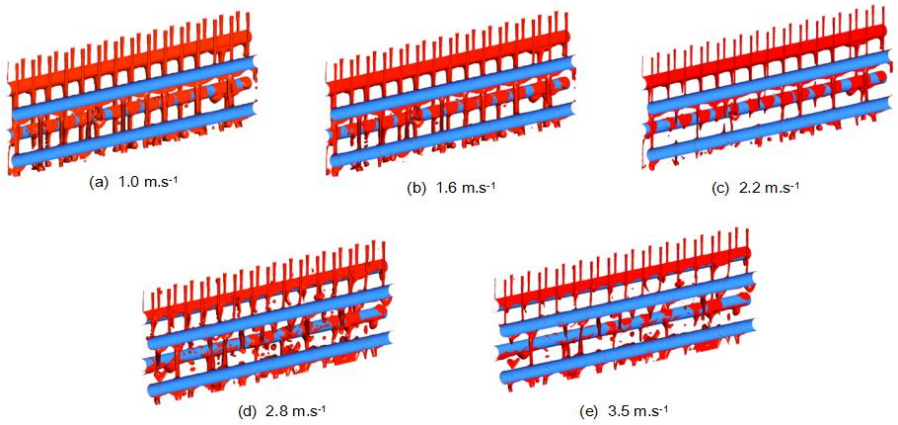

Figure 6: The influence of inlet air velocity on flow modes under the spray density of 0.060 kg·m^{-1}·s^{-1}

3.3 The effects of spray density (Γ) and inlet air velocity ($u_{a,in}$) on air temperature

The temperature distribution outside tubes can reflect the heat transfer process from water to air under different conditions. Figure 7 (a~b) show the temperature of water and air outside tubes under various Γ and $u_{a,in}$. Along the axial direction, the temperature is the highest at the falling film flow regions, while the air temperature between two adjacent spray water inlets is lower than other positions near the water droplet or column. Along the height direction, the air temperature increases greatly from the bottom up as given by the color change from blue to yellowish green. As presented in Figure8 (a~e), the average air temperature $T_{a,m}$ increase logarithmically along the height direction. The correlation between $T_{a,m}$ and height H is given by

$$T_{a,m} = a_0 \ln(H) + a_1 \tag{9}$$

where a_0 and a_1 are constant for specific Γ and $u_{a,in}$. With the increment of Γ, the wetting degree of tube surface increases, resulting from the transitions of flow mode from droplet to droplet-column and column as discussed earlier. The coefficient a_0 in the equation becomes greater with the rise of Γ, which indicates that the average air temperature ($T_{a,m}$) has a greater increase rate at large Γ. When increasing the $u_{a,in}$, not only the wetting degree of tube surface decreases, but also the air flow is capable of absorb more heat in a unit time due to the increase mass flow rate. Therefore, the $T_{a,m}$ has a smaller increase rate (smaller a_0) with the increase of $u_{a,in}$.

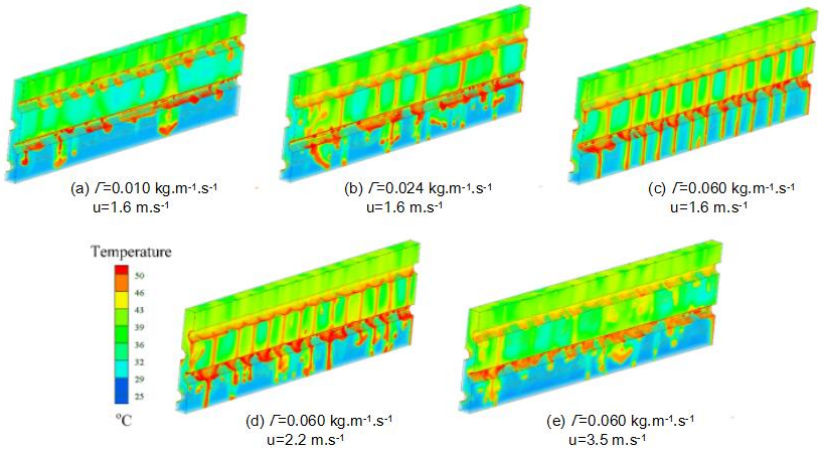

Figure 7: The temperature distributions under different spray density and inlet air velocity

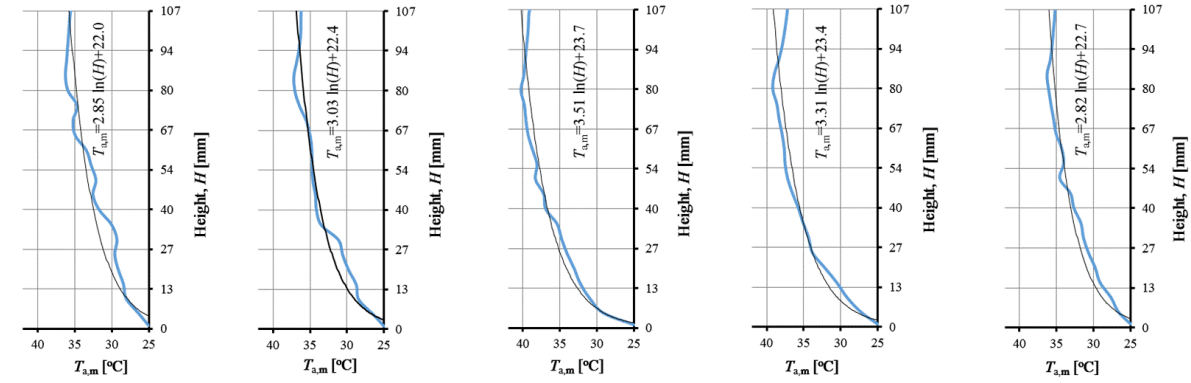

(a) Γ=0.010 kg·m^{-1}·s^{-1}, $u_{a,in}$=1.6 m·s^{-1} (b) Γ=0.024 kg·m^{-1}·s^{-1}, $u_{a,in}$=1.6 m·s^{-1} (c) Γ=0.060 kg·m^{-1}·s^{-1}, $u_{a,in}$=1.6 m·s^{-1} (d) Γ=0.060 kg·m^{-1}·s^{-1}, $u_{a,in}$=2.2 m·s^{-1} (e) Γ=0.060 kg·m^{-1}·s^{-1}, $u_{a,in}$=3.5 m·s^{-1}

Figure 8: The average air temperature along height direction under different spray density and inlet air velocity

4. Conclusions

This paper developed a three dimensional numerical model considered the air-water shear force and water evaporation in CWCT. With the VOF multiphase model, SST κ-ε turbulence model and user defined function, the 3-D distributions of flow mode, air temperature, the influence of $\Gamma$and $u_{a,in}$ were analyzed. The joint effect of $\Gamma$and $u_{a,in}$ can alter the falling film flow mode, under the spray density of 0.048 kg·m^{-1}·s^{-1} and 0.060 kg·m^{-1}·s^{-1} in which condition the Re_w is greater than 288, the falling film flow develops into column mode. The inlet air velocity can largely influence the flow mode in CWCT. The average air temperature increases from 25° to 35° along height direction, and their increase rates enlarge with the increment of Γ, but decrease with the increase of $u_{a,in}$.

Acknowledgments

Financial supports from the National Natural Science Foundation of China (No. U1462113, 21606261) and the Science and Technology Planning Project of Guangzhou city (No. 201704030136) is gratefully acknowledge

References

Smith, S.T., Hanbya, V.I., Harpham, C., 2011. A probabilistic analysis of the future potential of evaporative cooling systems in a temperate climate. Energ. Buildings. 43(2-3), 507-516.

Hasan, A., Siren, K., 2003. Performance investigation of plain and finned tube evaporatively cooled heat exchangers. Appl. Therm. Eng. 23(3), 325-340.

Chen, X., Shen, S., Wang, Y., Chen, J., Zhang, J., 2015. Measurement on falling film thickness distribution around horizontal tube with laser-induced fluorescence technology. Int. J. Heat Mass Tran. 89, 707–713.

Ding, Y., Bi, X., Wilkinson, D.P., 2013. 3D simulations of the impact of two-phase flow on PEM fuel cell performance. Chem. Eng. Sci. 100(30), 445-455.

Fiorentino, M., Starace, G., A numerical model to investigate evaporative condensers behavior at tube scale. 2014. In: ASME 2014-12th Biennial Conference on Engineering Systems and Analysis, Copenhagen, Denmark.

Fiorentino, M., Starace, G., 2016. Numerical investigations on two-phase flow modes in evaporative condensers. Appl. Therm. Eng. 96, 777-785.

Xie, X., Zhang, Y., He, C., Xu, T., Zhang, B., Chen, Q., 2017. Bench-scale experimental study on the heat transfer intensification of a closed wet cooling tower using aluminum oxide nanofluids. Ind. Eng. Chem. Res. 56(20), 6022-6034.

José, F.S., Ángel, Á.P., 2014. Refrigerant falling film evaporation review: Description, fluid dynamics and heat transfer, Appl. Therm. Eng. 64(1-2), 155-171.